

## **Hyperspectral Imaging of River Systems**

Curtiss O. Davis

College of Oceanic and Atmospheric Sciences

104 COAS Admin, Bldg

Corvallis, OR 97331

Phone: (541) 737-5707, fax: (541) 737-2064, email: [cdavis@coas.oregonstate.edu](mailto:cdavis@coas.oregonstate.edu)

Award Number: N000141010448

### **LONG-TERM GOALS**

The Navy has a requirement to rapidly and covertly characterize the coastal environment in support of Joint Strike Initiatives. Over the past 16 years we have demonstrated that spaceborne hyperspectral remote sensing is the best approach to covertly acquire data on shallow water bathymetry, bottom types, hazards to navigation, water clarity and beach and shore trafficability to meet those requirements. The long term goal of this work is to put a hyperspectral imager capable of making the appropriate measurements in space to demonstrate this capability.

### **OBJECTIVES**

The objective of this work is to put a hyperspectral imager in space to demonstrate the ability to covertly acquire data on shallow water bathymetry, bottom types, hazards to navigation, water clarity and beach and shore trafficability. Our work takes advantage of the Hyperspectral Imager for the Coastal Ocean (HICO) currently flying on the International Space Station (ISS). As HICO Project Scientist I work to enhance community awareness of the need for and utility of hyperspectral imaging of the coastal ocean. Our work includes advancing methods of on-orbit calibration and product validation, and processing and analyzing hyperspectral data of the coastal ocean. In particular in this study we are using HICO data to characterize the properties of river systems and coastal waters. Conventional ocean color sensors have 1 km pixels and a few spectral channels; these have not proven adequate to resolve the complexity of river systems. HICO was designed to sample the coastal ocean and has 95 m GSD and 88 spectral channels suitable to resolve river systems and other coastal features. To make the best use of this data we are developing algorithms and approaches for resolving the constituents of river plumes, harmful algal blooms and other complex systems.

In June 2010 the Korean Geostationary Ocean Color Imager (GOCI) was launched and it is providing the first ocean color imagery from geostationary orbit for a region around Korea, Japan and China. GOCI samples the region every hour (vs. once every few days for HICO) and is providing the first data suitable to resolve phytoplankton physiological responses, and coastal physical dynamics including tidal and plume dynamics on an hourly basis. This year we initiated work to create and test new algorithms for coastal products designed to take advantage of the high resolution data of HICO and GOCI. In particular, HICO, with its higher spatial and spectral resolution, allows a more accurate estimation of shallow water bathymetry and what is in the water column. While GOCI, with its hourly

sampling, enables estimation and modeling of coastal 'dynamics' --- how the murky coastal water is mixing and where it might be going next.

## **APPROACH**

Five tasks are planned for the four year period of this grant (FY2010-2013):

1. Develop, test and evaluate algorithms for deriving optical properties, chlorophyll, suspended sediments and CDOM for coastal systems including river systems. We will work with MERIS and HICO data and use the Columbia River system and adjacent coastal waters as a test area for this work.
2. Collect and analyze HICO data for the Yangtze River and adjacent coastal regions in China. Once we have developed the algorithms and approaches that work for the Columbia River we will test and evaluate those algorithms for the Yangtze and other river systems. The goal is to validate our algorithms and to further our understanding of this important river and the East China Sea which are rapidly changing due to the development of the Three Gorges Dam and continued urbanization of China.
3. Conduct a direct comparison of HICO and GOCI data for representative scenes in the GOCI imaging area. This will include Tokyo Bay, the Han and Yangtze Rivers and adjacent areas where HICO data is available. GOCI samples the entire region hourly, so if it is clear for the HICO data collection, we should have GOCI data within one hour for comparison. Comparison will include geolocation, radiometric and spectral calibration, and other properties to assure that we can use the two data sets together for the proposed analysis.
4. Using algorithms developed for HICO data that take advantage of its unique spectral properties, assess the detailed shallow water bathymetry and structure of the Han River delta and mud flats for available HICO scenes. Compare these results with GOCI data time series for the same time and develop algorithms for shallow water bathymetry using GOCI data. Then use the time series of GOCI data to follow the river dynamics and water depth changes over a day/tidal cycle.
5. Develop product algorithms that use HICO data to 'upscale' GOCI data spatially and spectrally. That is, attempt to create a 'merged' data products that have GOCI's temporal coverage, and HICO's spatial/spectral coverage.

## **WORK COMPLETED**

Our work is focused on the coastal ocean and a major issue for the coastal ocean is that the standard case 1 algorithms used to calculate chlorophyll and other water properties assume that phytoplankton with an associated level of Colored Dissolved Organic Matter (CDOM) and water itself are the only optically active components. In coastal waters high levels of CDOM from rivers and coastal runoff, large phytoplankton blooms, sediments from rivers, or resuspension from the bottom are all significant optical components that need to be considered as part of the optical signature (Davis, et al., 2007). For example the standard MODIS and MERIS products give false high chlorophyll values for the Columbia River Plume (**Fig. 1**). The MERIS neural network (algal 2) algorithms are designed for

European coastal waters and do a better job of separating chlorophyll and suspended sediments. We are working to modify them for Oregon coastal waters and eventually for use with HICO data. Note also that the 1 km MODIS data does not adequately sample the Columbia River mouth including the mixing zone that is order 50 km inland from the coast. MERIS 300 m data does a better job of imaging the estuary but HICO has 95 m GSD and full spectral data (88 channels covering the 400 – 900 nm spectral region) for this example river system.

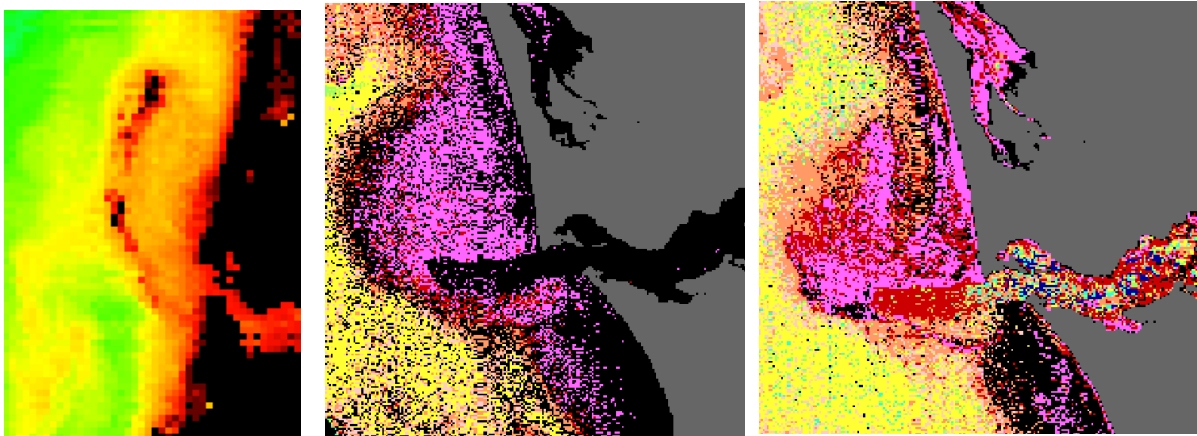


***Figure 1. Satellite ocean color images of the Columbia River estuary and plume on September 10, 2009. Left, is the MODIS standard 1000 m chlorophyll product. This algorithm gives false high values for the river system (red in this color scale) due to the high suspended sediments in the river water. The large pixels do not image the river mouth effectively. Center is the MERIS 300 m standard chlorophyll product (algal 1). The river mouth and near shore plume are black indicating the algorithm does not give a valid product for these waters and the results are masked out. Right is the MERIS neural network coastal chlorophyll product (algal 2) which shows reasonable chlorophyll values for the river mouth and nearshore plume. The 300 m MERIS pixels do a much better job of imaging the river mouth.***

The Hyperspectral Imager for the Coastal Ocean (HICO; Lucke et al. 2011; Corson and Davis, 2011) is an imaging spectrometer based on the PHILLS airborne imaging spectrometers (Davis et al. 2002). HICO is the first spaceborne imaging spectrometer designed to sample the coastal ocean. HICO samples selected coastal regions at 95 m with full spectral coverage (400 to 900 nm sampled at 5.7 nm) and a high signal-to-noise ratio to resolve the complexity of the coastal ocean. HICO is sponsored by the Office of Naval Research as an Innovative Naval Prototype (INP), to demonstrate coastal products including water clarity, bottom types, bathymetry and on-shore vegetation maps. As an INP, HICO also demonstrates innovative ways to reduce the cost and schedule of this space mission by 80% by adapting proven PHILLS aircraft imager architecture and using Commercial Off-The-Shelf (COTS) components where possible.

The HICO program was initiated in February 2006. In January 2007 HICO was selected to fly on the Japanese Experiment Module Exposed Facility (JEM-EF) on the International Space Station. Construction began following the Critical Design Review on November 15, 2007. HICO was completed in July 2008 and it was integrated into the HICO and RAIDS Experimental Payload (HREP) in August 2008. HICO is integrated into HREP and flown with support and direction from DOD's

Space Test Program. HREP was launched on the Japanese H-2 Transfer Vehicle (HTV) September 10, 2009. The HTV rendezvoused with the ISS on September 17, 2009. HICO was installed on September 23 and collected its first images on September 24, 2009. To date over 6000 HICO scenes have been collected, processed to level 1b and archived. The research community can access HICO data through the OSU HICO website: <http://hico.coas.oregonstate.edu>.

For the past three years we have been collecting HICO™ data for the Columbia (**Fig. 2**) and Yangtze Rivers (**Fig. 3**). There are many constraints on data collection with this demonstration instrument including being limited to one image per orbit for data transmission, gaps due to the ISS orbit and operations and clouds. However, we now have a number of good images for both rivers and are continuing to collect imagery at both locations.

Yangtze River in China is a major source of sediments and nutrients to the China Sea and Straits of Taiwan. In a comparison of chlorophyll products from MODIS and HICO™ (**Fig. 3**) we see the big picture in the MODIS data, but far more detail in the HICO™ data. Also, note that the MODIS algorithms fail over waters with high sediments, but the HICO™ data is not saturated and the HICO™ algorithm returns useful data even in these high sediment waters. After on-orbit vicarious calibration (Gao et al, 2012) the at sensor radiances are very close and where the MODIS data is not saturated the match of chlorophyll values is very good.



***Figure 2. Pseudocolor image of the Columbia River mouth and adjacent coastal waters made with 3 channels of HICO data. The 90 m HICO data shows many more details including shallow bars in the river, the bridge from Astoria Oregon across to Washington, breakwaters and the complex mixing patterns as the plume moves offshore. HICO™ is a trade mark of the US Naval Research Laboratory.***

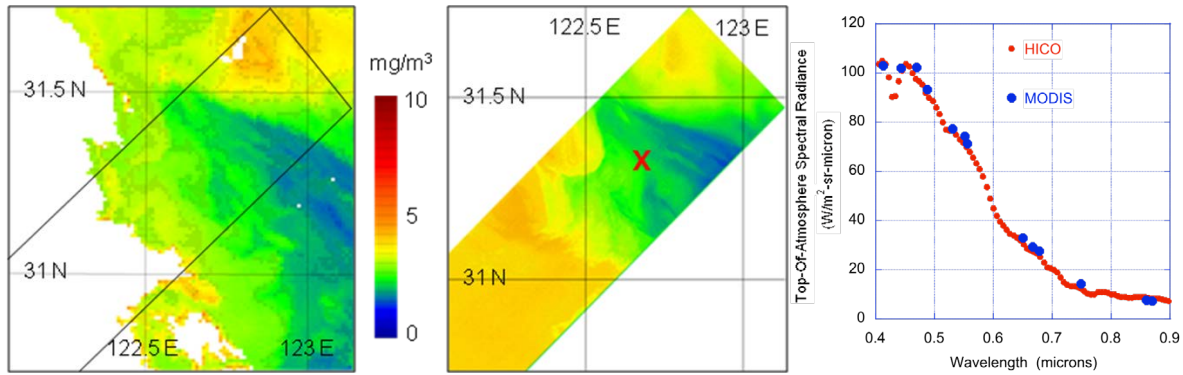


**Figure 3.** Nearly coincident MODIS and HICO<sup>TM</sup> images of the Yangtze River, China taken on January 18, 2010. Left, MODIS image (0500 GMT) of Chlorophyll-a Concentration (mg/m<sup>3</sup>) standard product from GSFC. White areas are regions where sensor channels saturated and the algorithm failed to produce a product. The box indicates the location of the HICO image relative to the MODIS image. Middle, HICO image (0440 GMT) of Chlorophyll-a Concentration (mg/m<sup>3</sup>) from HICO data using ATREM atmospheric correction and a standard chlorophyll algorithm. Right, comparison of the at sensor radiances from HICO (red) and MODIS (blue) for location X in HICO image showing the accurate on-orbit calibration for HICO (Gao, et al, 2012).

To validate MERIS and HICO data products for the Oregon Coast we have been collecting profiles of downwelling irradiance and upwelling radiance using a Satlantic HyperPRO (Fig. 4). The HyperPRO is a free falling optical profiling system that collects profiles of spectral Lu and Ed and chl fluorescence, backscatter, T and salinity. The system is calibrated by Satlantic and we use the Satlantic software for processing including all of the latest corrections based on NIST calibrations.

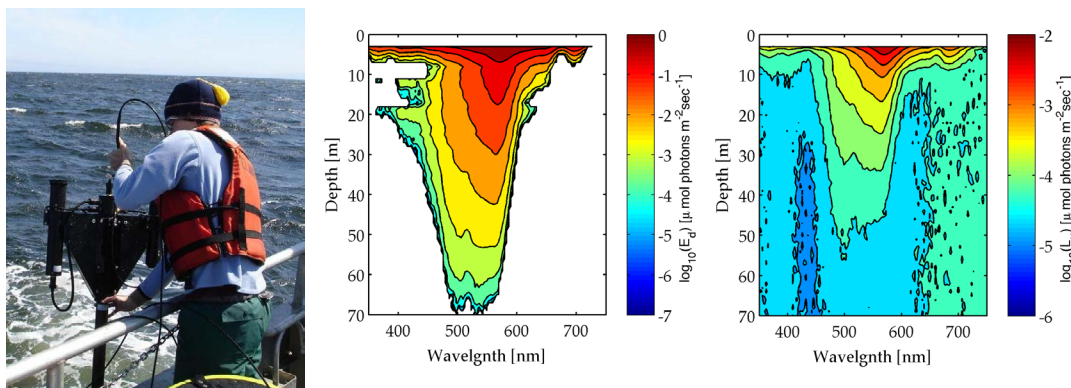


**Figure 4.** Collecting HyperPRO data and an example data set from the MILOCO cruise off the Oregon coast taken June 4, 2009. (Left side of the figure shows a research associate lowering the HyperPRO instrument over the side of a small research vessel. The center panel shows the depth profile of the spectra of downwelling irradiance. The right panel shows the depth profile of the spectra of the upwelling radiance collected with the HyperPRO instrument.)

This system produces high quality measurements of spectral remote sensing reflectance (Rrs) for direct comparison to the HICO data after atmospheric correction. The HyperPRO data together with other data collected on each station including HPLC pigments, productivity, CDOM, suspended sediments are placed in the MILOCO data base with web access.

A key focus of our effort is to differentiate the river plume, Harmful Algal Bloom (HAB), or other key spectral feature from the background signal and to find a rapid way of processing the data to produce a river plume product. While standard methods exist for atmospheric correction of land (Gao, et al. 1993) and open ocean (Gordon and Wang, 1994) data atmospheric correction of coastal ocean data remains problematic. With that in mind our method uses techniques that do not need atmospheric correction, but start directly with the calibrated at-sensor radiances.

The basic idea for the indicator methods is to first estimate what a typical 'dark pixel' spectrum for a region of interest, and second (after subtracting this 'typical dark pixel') to examine the sensitivity of the residual spectrum, including spectral derivatives, to target products --- sediment, chlorophyll, or sampled pixels know to contain pigments of interest, such as phycocyanin commonly found in cyanobacteria associated with HABs. That is, the indicators are meant to be 'fingerprints' for the target product (Bustillos-Guzman et al. 2004).

The starting point is converting the at-sensor radiance data to a normalized reflectance by converting to the apparent at-sensor reflectance. This is computed using the Naval Research Lab's tafkaa\_6s code (Gao, et al. 2000) according to the formula:

$$\rho_{obs}^* = \frac{\pi L_t}{\mu_0 E_0} \quad (1)$$

where  $L_t$  is the observed radiance,  $E_0$  is the solar irradiance, and  $\mu_0$  is the cosine of the solar zenith angle. Next we create a reference spectrum for each image. More specifically, we try to estimate a dark ocean pixel from looking at the sensor radiance,

$$r_{obs}^*(l) = r_a(l) + t r_w(l) \quad (2)$$

where  $r_a$  accounts for atmospheric and sea-surface reflection,  $r_w$  picks up contributions below the water surface, and  $t$  denotes the transmittance from the water surface to sensor. In developing 'indicator maps,' we consider a slightly different decomposition. Namely, we start by imagining, at every pixel, the at-sensor radiance we would see if the water was clear; a so-called dark water pixel. This is an 'idealized' quantity, but the difference between this ideal radiance signal, and the observed signal at sensor, provides information about what is in the water, which is relatively independent of what is in the atmosphere. Thus it is a good starting point for creating an 'indicator' function for what is in the water.

In our approach a dark water pixel will be defined 'empirically,' based on an image, or collection of images, of a region of interest, and choosing pixels, or patches of pixels, which determine 'dark water,' or water free of river plume materials, or other features of interest, for that region. So in practice, the dark water pixel could contain some background material in the water column that we will consider as 'clear water,' or a dark water pixel, which is typical for the region. We call this type of pixel, which contains some below water signal, a regional dark pixel, but in the following discussion we will refer to it as a dark pixel. It is the background signal from which we start any further signal processing.

Mathematically we can write this decomposition as:

$$r^*_{\text{obs}}(\lambda) = r_a(\lambda) + t (r_d(\lambda) + r_b(\lambda)) \quad (3)$$

$$= r_M(\lambda) + r_I(\lambda) \quad (4)$$

where  $r_M(\lambda)$  is the modeled spectrum, and  $r_I(\lambda)$  is the ‘indicator’ spectrum, it is simply the residual between the at sensor radiance minus any modeling we do for the spectrum (Tufillaro and Davis 2010). If  $r_M$  is chosen as a dark pixel in the scene than it is what is normally referred to as ‘dark pixel subtraction’, a very simple but often effective scheme for atmospheric correction. The terms  $r_d(\lambda)$  and  $r_b(\lambda)$  are called the ‘dark water’ and ‘bright water’ contributions to  $r_w(\lambda)$  respectively. The trick to this approach is finding (a typically empirical) model of dark pixel spectra that allow us to create a data based decomposition of  $r^*_{\text{obs}}(\lambda)$  to identify one or more dynamic water constituents of interest.

In the visible spectrum the dominant spectral feature is Rayleigh scattering which has the spectral form of a negative power function. To create an empirical model to fit the ‘dark water’ pixels we take a guess at the following functional form:

$$r_M(\lambda_n) = (a + b(\lambda_n - \lambda_1))^{-4} \quad (5)$$

where  $a$  and  $b$  are model parameters which are to be estimated from the spectral data  $\lambda_n$  and  $r_M(\lambda_n)$  and  $\lambda_1$  is the first value of the wavelength in data set being modeled, a constant. In HICO L1b data sets, each at-sensor pixel has 88 radiance values between 400 nm to 900 nm. The typical scene size covers approximately 42 km by 190 km, and 500 by 2000 pixels. To ‘model’ the data we limit our sets to wavelengths between 450 nm to 900 nm, so in our data sets  $\lambda_1 = 450$  nm and  $\lambda_N = 900$  nm. We have applied it to the Columbia River and Yangtze River HICO images using it to differentiate the plume features. Those results are shown in the results section below.

The next step is to take the radiances (less dark pixels), compute its derivatives, and then create a map (typically just a nonlinear regression) from the reflectance data ( $r_w$ ,  $dr_w/d\lambda$ ,  $d^2r_w/d^2\lambda$ , ...) to our target product, either pixels in the scene known to contain the product of interest or the spectra of in-situ above water radiances for the site (Tufillaro, Davis, and Ortiz 2011). In practice we often compute the ‘principal components’ of the spectral signal first, and use these to create the indicator map following the procedure recently described by Ortiz et al. (Ortiz et al. 2011). The principal components are spectral decomposition of the signal which breaks the signal into its empirical modes producing the greatest variance. In this way we can both reduce the dimension of the map, as well as pick out the parts of the signal which are best correlated to changes across the scene.

The use of derivative data, in addition to the original spectral radiances is helpful since it can highlight significant features. This observation has been used often in the past for identification of laboratory spectra, and it is possible to directly adapt laboratory identification methods, such as derivative spectroscopy, to remote sensing product estimation. Derivate spectroscopy has previously been used to identify optimal spectral channels for the design of multi-spectral instruments (Lee et al. 2007), and to estimate coastal bottom types from aerial hyperspectral data (Louchard et al. 2002). Here we illustrate the use of methods adapted from derivative spectroscopy for product generation from HICO data. Derivate spectroscopy methods are useful in untangling spectral components when the underlying scattering or absorptive features have significantly different half widths. Consider the sketch of a simple at-sensor spectrum shown in **Fig. 5**. The broadest feature is the Rayleigh scattering which is the

monotonically decreasing across the spectrum from blue to red. Taking the first derivative de-emphasizes this broad scattering signature by essentially subtracting a baseline from initial spectrum.

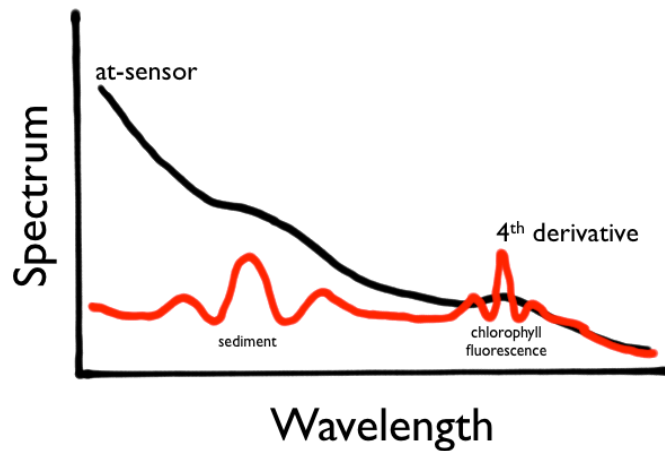


**Figure 5.** Sketch of a typical HICO spectrum showing how derivative spectroscopy can amplify narrow-band features in spectrum. The 4th derivative of the spectrum in red shows how the fourth derivative is much more sensitive to narrow spectral features, such as chlorophyll fluorescence.

Features seen include a signal in the yellow part of the spectrum with a relatively board bandwidth, and a signal in the red (685 nm) for chlorophyll fluorescence with a narrower bandwidth. The detection of these underlying absorptive and fluorescent signatures can be sharpened by the use of derivative spectroscopy. Specifically peaks with narrower half-widths grow more quickly with the order of the derivative. This is illustrated in **Fig. 6** where we show that the derivative helps to highlight signatures sensitive to sediment in recent Columbia River spectra. Spectral features identified in this way can create products which are 'regionally tuned,' and built on historical data specific to a coastal area.

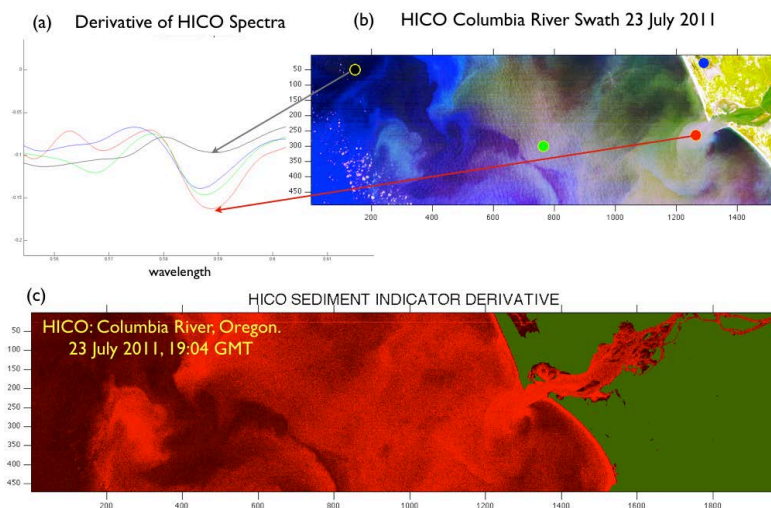


**Figure 6.** Analysis of a HICO spectra using derivative spectroscopy. (a) The derivative spectra calculated at the points indicated in the HICO image (b) taken 23 July 2011. (c) A 'regionally tuned' map of sediment concentration (bright red is high sediment, dark red low) emanating from the Columbia River. The derivative at 540 nm is highly sensitive to the sediment in the river plume.

The method for our sediment and pigment products from HICO is similar to that recently described by Gitelson, et al. (2011). They used HICO data to create regionally tuned chlorophyll-a product for the Azov Sea, where they pick the bands for the product, starting with all the HICO wavelengths, and then optimizing the choice of bands, for a band-ratio algorithm, based on in-situ data. Their method is also informed by derivative analysis in their choice of the final bands for the regression. Our method differs in that we build our optimization using all the HICO wavelengths, and instead of testing for the sensitivity to specific bands, rather, our sensitivity is based on the principal components which are a linear combination of all the wavelengths. Specifically, the method we describe could contain details about the spectral shape - such as spectral bandwidths - which might not be utilized in the method of Gitelson and co-workers.

Additionally as HICO project scientist, I am funded by NRL to continue to work with the engineers and scientists at NRL and partner institutions to prepare for the processing and analysis of HICO data. The NRL team processes the HICO data to standard level 1b (calibrated at sensor radiances) products. At OSU we archive and distribute HICO data for academic users and international partners (Davis et al. 2012). We are also processing the data on a request basis providing some L3 products with geolocation and atmospheric correction, as well as collaborating with a number of partners to use HICO data as part of their on-going programs.

## RESULTS

The focus of this effort is on the processing and analysis of HICO data to demonstrate the utility of hyperspectral imaging for characterization of coastal waters. Our efforts are particularly focused on river systems and we have conducted initial analysis of HICO data for the Columbia and Yangtze Rivers. To date we have also processed an extensive set of MERIS data for the Columbia River and Oregon Coastal Waters. And we have collected *in situ* data for validation of products off the Northwest Coast and are currently comparing the MERIS and HICO products with that *in situ* data.

An example of the where we have applied the derivative analysis plume indicator approach described above is shown in **Fig. 7** for HICO images of the Columbia River. More recently, we began work with Alex Kurapov (Physical Oceanography, Oregon State University) on how to assimilated ocean color data of the Columbia River plume from both MERIS and HICO into Alex's groups regional ocean model for forecasting off the Oregon Coast (Kurapov et. al 2011). This work should allow us to make short term forecasts of water clarity and turbidity in the region of the Columbia River mouth, and to follow the fine details (temporally and spatially) of the wanderings of the river plume.

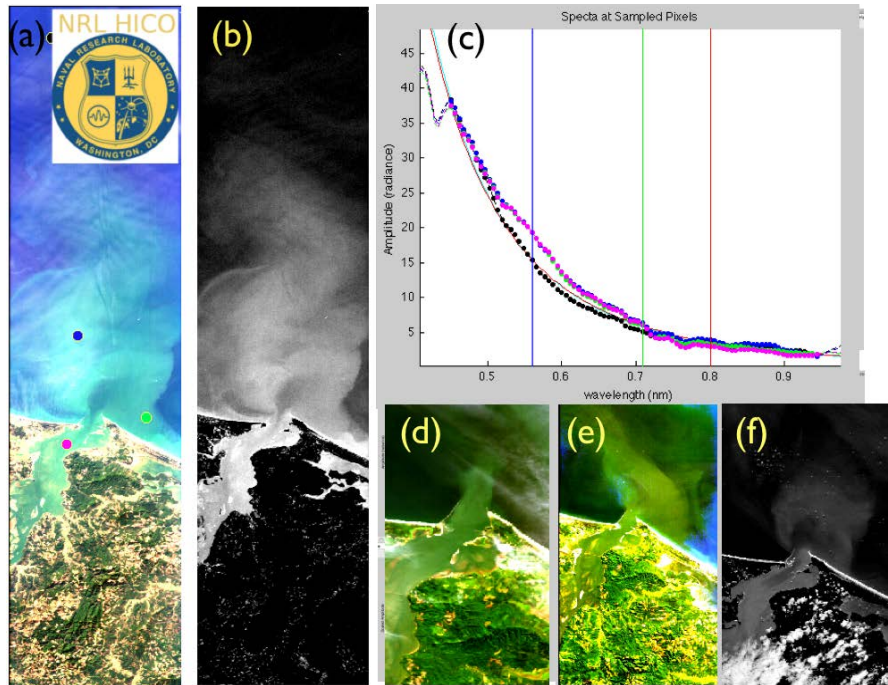


**Figure 7. Images of Columbia River with indicator map highlighting sediments: (a) L1B HICO<sup>TM</sup> image of Columbia River mouth 19 March 2010. (b) An indicator for sediments in the Columbia River based on the dark pixel spectral separation for the image presented in Fig. 3(a). (c-f) Typical spectra and sediment indicator maps for three HICO images from July 2010.**

Similarly we have applied this technique to HICO images of the Yangtze River in China. **Fig. 8** shows a sequence of clear images from HICO along with typical plots of the second derivative of the spectrum with respect to wavelength. The wavelengths around 620 are sensitive to sediment concentrations (and 580 is a chlorophyll absorption minimum), and MERIS uses a 620 nm channel to estimate sediment. As also pointed out by Gitelson et. al. (2011), HICO allows us to tune the product algorithm wavelengths to the products for a particular region. In the Yangtze region, which can exhibit extremely high sediment concentrations, the sediment maximum occurs closer to 610 nm rather than 620nm, and our principal component method, like optimized band ratio methods (Gitelson et. al., 2011), will weigh the sediment product algorithm more closely to the sediment maximum when trained on regional data (**Fig. 9**).

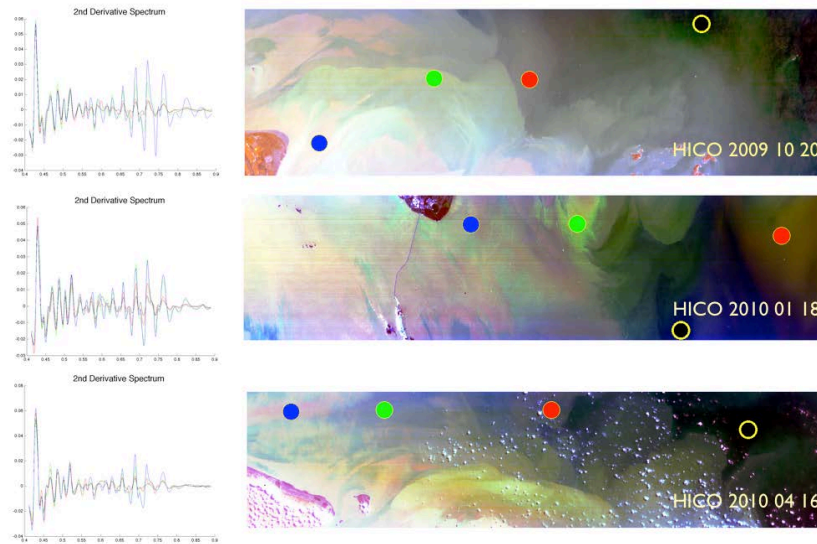


**Figure 8. HICO images and derivative spectra of the Yangtze river in China. Using collections of images we are building up signatures to distinguish the constituents of the water column for this region.**

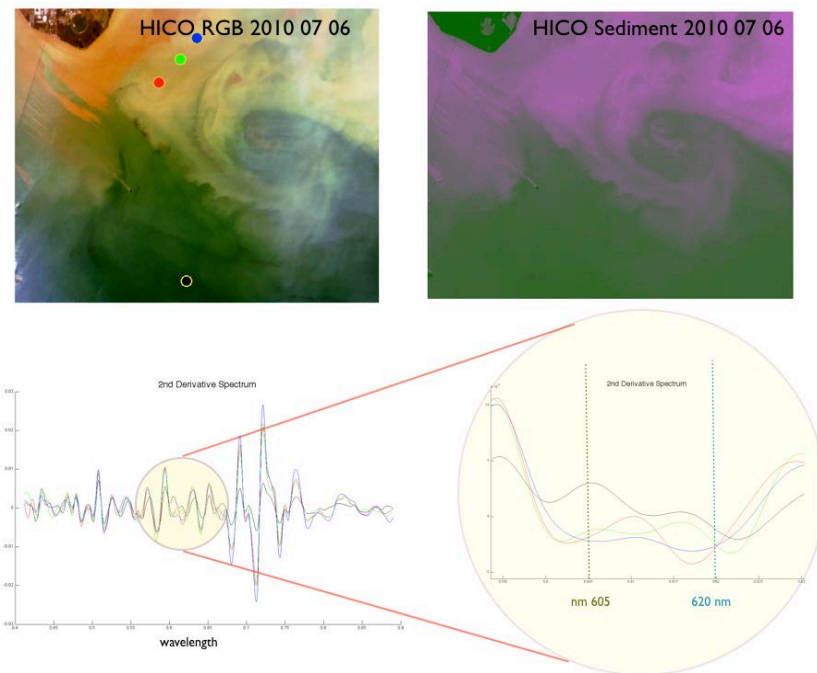


**Figure 9. Upper left, HICO RGB image and, upper right, sediment product map for Yangtze River, China on 6 July 2010. Lower, the second derivative of the spectrum indicates that wavelenths around 605 nm are much more sensitive to sediment concentration than the 620 nm MERIS band 6. Our HICO product algorithm will automatically optimize the product algorithm to weight data more heavily to around 605 nm when trained on Yangtze regional historical data, like that presented in Fig. 8.**

As mentioned, HICO has approximately 100 meters spatial resolution and 5.7 nm spectral resolution. GOCI is 500 m multispectral but has hourly coverage. To create ‘merged’ GOCI-HICO data that approach GOCI’s temporal resolution and HICO’s spatial resolution, we are attempting to create a super-resolution spatial filter for GOCI based on HICO data around the Han River. The algorithm was recently created by (Charles et al, 2011) and is based on sparse signal processing.

The sparse filter model for the hyperspectral data computes an observed spectrum at each pixel,

$$x_{ij} = \sum \phi_k a_{i,j,k} + \epsilon_{ij} = \Phi \mathbf{a}_{i,j} + \epsilon_{i,j}$$

where  $\Phi \in R^{M \times N}$  is a matrix of basis functions (called ‘dictionary elements’) and  $\mathbf{a}_{i,j} \in R^N$  is the coefficient vector for the pixel  $\{i, j\}$ .  $\epsilon_{i,j}$  is the noise term. The model is a linear mixing model, but it is not the more common principal components model in which the coefficients sum to one. The optimization procedure to estimate the coefficients is a nonlinear process that explicitly assumes a ‘sparsity’ assumption --- that each pixel contains only a few distinct materials. The coefficient’s are estimated for each pixel by a  $\ell_1$  regularized least-squares optimization termed Basis Pursuit De-Noising (Chen et. al., 2001).

The trick, of course, is the find a dictionary which corresponds to the materials in the waters of a specified region. To do this we use hyperspectral data from HICO for pixel collections from distinct water masses (see **Fig. 10**) and attempt to find a sparse coding model from the GOCI data by performing an inverse solution of the Basis Pursuit. In other words, we solve an optimization problem that seeks hyperspectral coefficients that are consistent with the sparsity assumption and with data from GOCI and HICO. Initial results are shown in **Fig. 10**. The dictionary learning appears to create basis functions that resemble open water, sediment rich, and near-shore spectra. However, to date, we do not think the algorithm has uniquely identified spectra for specific materials in the water column. We are currently adapting the algorithm to do a weighted optimization to attempt to force it into more physically unique spectra.

HICO has been operating on the ISS for three years. Over 6000 images have been collected for locations around the world. HICO is operating as planned and the data products look very good. We continue to work with the NRL team on the on-orbit calibration and validation of HICO data. As Project Scientist it is my goal to work with the scientific community to make the best possible use of this unique data set. To that end we operate the HICO website at OSU (<http://hico.coas.oregonstate.edu>) which serves data to interested scientists around the world. We currently have over 50 users; 23 of them have submitted formal proposals and their projects are summarized on the HICO website (Davis et al, 2012). The website also includes publications and presentations on HICO, an archive of existing data and a tool for selecting sites and requesting data as well as directions for working with the data and products. A first HICO international team meeting was held at the Ocean Optics Conference in Glasgow, Scotland, October 10, 2012 and the presentations and results will be posted on the HICO website later in October.

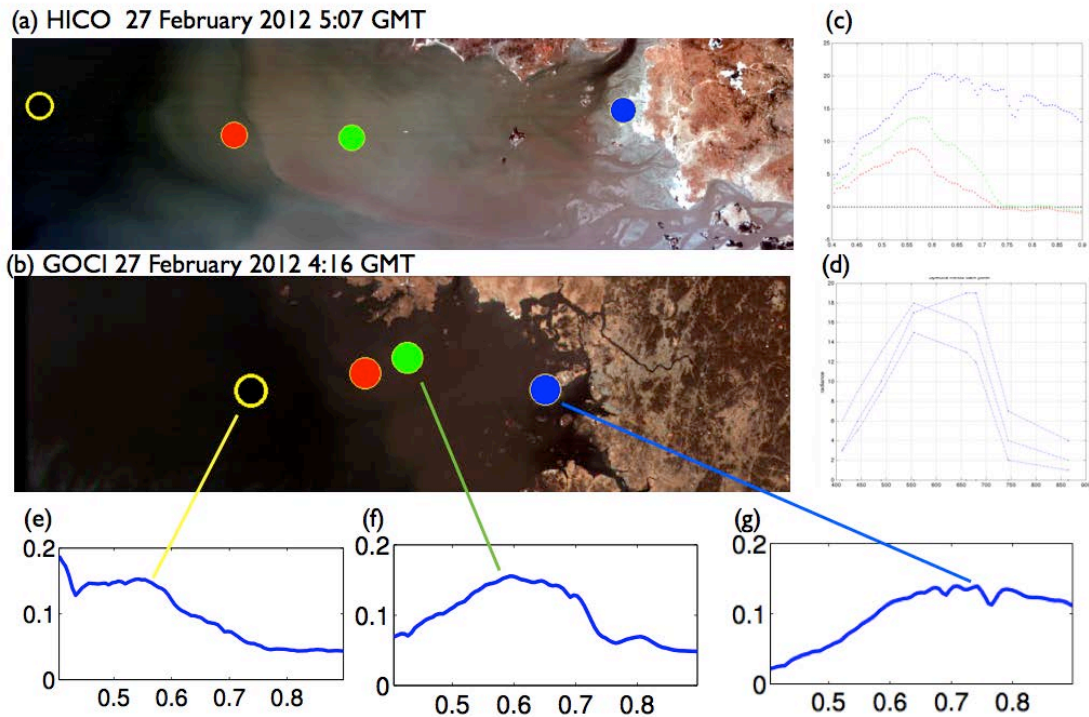


**Figure 10. Coincident HICO and GOCI data around the Han River, Korea. (a) HICO image, (b) GOCI image, (c)-(d) respective atmospherically corrected spectra, (e)-(g) learned dictionary elements, black: open water; green: sediment rich; blue: near shore (Joint work with Adam Charles, Georgia Tech, 2012).**

I have continued to support the Naval Research Laboratory in improving the calibration and on-orbit performance of HICO. This work led to two publications, one led by Bo-Cai Gao at NRL on the on-orbit calibration of HICO (Gao, et al, 2012; and see **fig. 3** above), and one in collaboration with Chuanmin Hu (U. south Florida) and others on the SNR requirements and performance of instruments on orbit. The procedure developed in Hu et al (2012) makes it possible to assess the performance of any sensor on orbit, and in particular HICO was compared to Hyperion a NASA experimental sensor designed for land imaging (**fig. 11**). This analysis confirmed that HICO achieved the planned SNR on orbit and our earlier analysis of HICO's on-orbit performance.

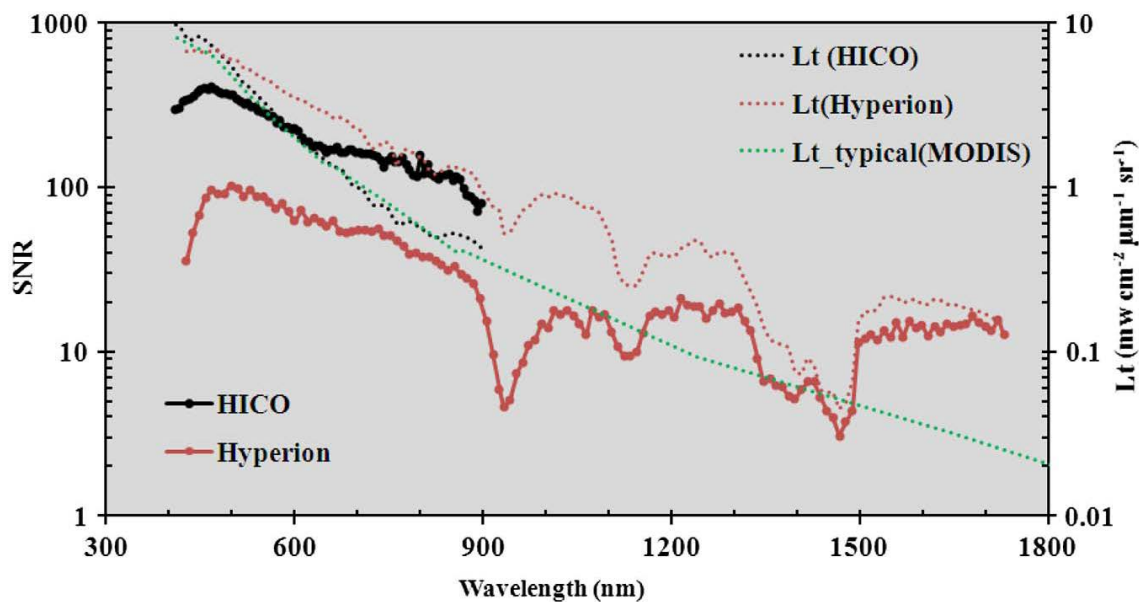


*Figure 11. SNR values were determined from hyperspectral instruments of HICO (black symbols) and Hyperion (brown symbols), respectively. While the input radiance used to determine HICO SNR is similar to  $L_{\text{typical}}$  for MODIS (green line), the input radiance used to determine Hyperion SNR is higher than MODIS  $L_{\text{typical}}$  in the green, red, NIR, and most shortwave IR wavelengths. [The plot covers the spectral region from 300 to 1800 nm. The left-hand scale is a log scale of SNR ranging from 1 to 1000. The HICO SNR ranges from 400 at 450 nm to 200 at 850 nm. The Hyperion SNR is approximately  $\frac{1}{4}$  of the HICO SNR.]*

## IMPACT/APPLICATIONS

The long term goal of this work is demonstrate the value of a hyperspectral imager capable of making the appropriate measurements from space to demonstrate the capability of this technology for the rapid and covert characterization of the coastal ocean to support naval operations around the world. We are using data from HICO on the ISS to demonstrate that capability. The work completed this year is another incremental step towards that goal.

## RELATED PROJECTS

We continue to collaborate regularly with colleagues at the NRL Remote Sensing Division (Code 7200; Jeff Bowles and others) and the NRL Oceanography Division (Code 7300; Rick Gould and others), Bob Arnone (U. Southern Miss.) and Zhong-Ping Lee (U. Mass. Boston).

## REFERENCES

Bustillos-Guzman, J., I. Garate-Lizarraga, D. Lopez-Cortes, F. Hernandez-Sanoval, 2004, "The use of pigment fingerprints in the study of harmful algal blooms," Rev. Biol. Trop. 52 Suppl 1:17:26.

- Corson, M. and C. O. Davis, "The Hyperspectral Imager for the Coastal Ocean (HICO) provides a new view of the Coastal Ocean from the International Space Station," AGU EOS, V. 92(19): 161-162.
- Charles, A., et., 2011, Learning sparse codes for hyperspectral images," IEEE Journal of Selected Topics in Signal Processing, 5(5): 963-978.
- Chen, et. al., 2001, Atomic decomposition by basis pursuit, SIAM Review 43 (1), 129-159.
- Davis, C. O., et al., 2002, Ocean PHILLS hyperspectral imager: design, characterization, and calibration, *Optics Express*, 10(4): 210-221.
- Davis, C.O., M. Kavanaugh, R. Letelier, W. P. Bissett and D. Kohler, 2007, Spatial and Spectral Resolution Considerations for Imaging Coastal Waters, *Proceedings of the SPIE* V. 6680, 66800P:1-12.
- Davis, C. O., J. Nahorniak and N. Tuffiaro, 2012, "Hyperspectral Imager for the Coastal Ocean (HICO) on the International Space Station: Three Years and Counting," *Proceedings of Ocean Optics XXI*, Glasgow, Scotland, October 7-12, 2012. [Extended abstract]
- Gao, B.-C., K. H. Heidebrecht, and A. F. H. Goetz, 1993, Derivation of scaled surface reflectances from AVIRIS data, *Remote Sens. Env.*, 44, 165-178.
- Gao, B.-C., M. J. Montes, Z. Ahmad, and C. O. Davis, 2000, An atmospheric correction algorithm for hyperspectral remote sensing of ocean color from space, *Appl. Opt.* 39(6): 887-896.
- Gordon, H. R., and Wang, M., 1994, Retrieval of water leaving radiance and aerosol optical thickness over the oceans with SeaWiFS: a preliminary algorithm, *Appl. Opt.*, 33, 443-452.
- Gitelson, A. A., B-C Gao, R-R Li, S. Berdnikov, and V. Saprygin, 2011, "Estimation of chlorophyll-a concentration in productive turbid waters usin a Hyperspectral Imager for the Coastal Ocean --- The Azov Sea case study, *Environ. Res. Lett.* doi:10.1088/1748-9326/6/2/024023.
- Kurapov, A. L., D. Foley, P. T. Strub, G. D. Egbert, and J. S. Allen, 2011: Variational assimilation of satellite observations in a coastal ocean model off Oregon, *J. Geophys. Res.*, 116, C05006, doi:10.1029/2010JC006909
- Lee, Z-P., K. Carder, R. Arnone, and M-X He, 2007a, Determination of primary spectral bands for remote sensing of aquatic environments, *Sensors* 7: 3428-3441.
- Louchard, E. M., R. P. Reid, C. F. Stephens, C. O. Davis, R. A. leathers, T. V. Downes and R. Maffione, 2002, Derivative analysis of absorption features in hyperspectral remote sensing data of carbonate sediments, *Optics Express*, 10(26): 1573-1584.
- Lucke, R. L., M. Corson, N. R. McGlothlin, S. D. Butcher, D. L. Wood, D. R. Korwan, R.-R. Li, W. A. Snyder, C. O. Davis, and D. T. Chen, 2011, "The Hyperspectral Imager for the Coastal Ocean (HICO): Instrument Description and First Images," *Applied Optics*, V. 50 (11): 1501-1516 doi:10.1364/AO.50.001501.
- Montes, M. J., B-C. Gao and C. O. Davis, 2004, "NR Atmospheric Correction Algorithms for Oceans: *Tafkaa* User's Guide." NRL Report: NRL/MR/7230-04-8760.
- Ortiz, JD, Witter, DL, Ali, KA, Fela, N, Duff, M, and Mills, L, 2011, Evaluating multiple color producing agents in Case II waters, *Int. J. Remote Sensing*, to appear.

Tufillaro, N., and C. O. Davis, 2010, "Indicators of plumes from HICO," *Proceedings of Ocean Optics XX*, Anchorage, AK, Sept 27 – Oct 1.

Wilson, T., and C. O. Davis, 1999, The Naval EarthMap Observer (NEMO) Satellite, *Proceedings of the SPIE*, **3753**, 2-11.

## PUBLICATIONS

Gao, B-C, R.-R. Li, R. L. Lucke, C. O. Davis, R. M. Bevilacqua, D. R. Korwan, M. J. Montes, J. H. Bowles and M. R. Corson. 2012, "Vicarious calibrations of HICO data acquired from the International Space Station," *Applied Optics*, V. 51 (14): 2559-2567. [Reviewed, published]

Hu, C., L. Feng, Z-P. Lee, C. O. Davis, A. Mannino, C. McClain, and B. Franz, 2012, "Dynamic range and sensitivity requirements of satellite ocean color sensors: learning from the past," *Applied Optics*, V. 51(25): 6045-6062. [Reviewed, published]

Davis, C. O., J. Nahorniak and N. Tufillaro, 2012, "Hyperspectral Imager for the Coastal Ocean (HICO) on the International Space Station: Three Years and Counting," *Proceedings of Ocean Optics XXI*, Glasgow, Scotland, October 7-12, 2012. [Extended abstract]

Davis, C. O., N. B. Tufillaro, M. Corson, B-C. Gao, J. Bowles, and R. Lucke, 2012, "HICO On-Orbit Performance and Future Directions," *Proceedings of Optical Remote Sensing of the Environment (ORSE)*, Monterey, CA, June 25, 2012, Optical Society of America. [Published abstract]

Davis, C. O., N. B. Tufillaro, M. Corson, B-C. Gao, and R. Lucke, 2012, "Hyperspectral Imager for the Coastal Ocean (HICO): overview and Coastal Ocean Applications," *Ocean Sciences Meeting*, Salt Lake city, UT, February 20-24, 2012. [Published abstract]

Davis, C. O., N. B. Tufillaro, and J. Nahorniak, 2012, "Eight years of Phytoplankton and Columbia River Plume dynamics from MERIS data," *Proceedings of the Eastern Pacific Ocean Conference*, timberline, OR, September 19-21, 2012. [Invited presentation]

Ryan, J. P., N. B. Tufillaro, and C. O. Davis, 2012, "HICO Observations of Biological and Sediment-Transport Processes in Monterey Bay, California," *Proceedings of Optical Remote Sensing of the Environment (ORSE)*, Monterey, CA, June 25, 2012, Optical Society of America. [Published abstract]

Tufillaro, N. B., and C. O. Davis, 2012, "Derivative spectroscopy with HICO," *Proceedings of Optical Remote Sensing of the Environment (ORSE)*, Monterey, CA, June 25, 2012, Optical Society of America. [Published abstract]